

Received:
19 June 2020Revised:
18 November 2020Accepted:
18 November 2020<https://doi.org/10.1259/bjr.20200780>

Cite this article as:

Daubert MA, Tailor T, James O, Shaw LJ, Douglas PS, Koweek L. Multimodality cardiac imaging in the 21st century: evolution, advances and future opportunities for innovation. *Br J Radiol* 2020; **94**: 20200780.

BJR 125TH ANNIVERSARY: REVIEW ARTICLE

Multimodality cardiac imaging in the 21st century: evolution, advances and future opportunities for innovation

¹MELISSA A DAUBERT, MD, ²TINA TAILOR, MD, ²OLGA JAMES, MD, ³LESLEE J SHAW, PhD, ¹PAMELA S DOUGLAS, MD and ²LYNNE KOWEEK, MD

¹Division of Cardiology, Department of Medicine, Duke University Medical Center, Durham, North Carolina, USA

²Division of Cardiothoracic Imaging, Department of Radiology, Duke University Medical Center, Durham, North Carolina, USA

³Department of Radiology, Cornell Medical Center, New York, New York, USA

Address correspondence to: Dr Melissa A Daubert

E-mail: melissa.daubert@duke.edu

ABSTRACT

Cardiovascular imaging has significantly evolved since the turn of the century. Progress in the last two decades has been marked by advances in every modality used to image the heart, including echocardiography, cardiac magnetic resonance, cardiac CT and nuclear cardiology. There has also been a dramatic increase in hybrid and fusion modalities that leverage the unique capabilities of two imaging techniques simultaneously, as well as the incorporation of artificial intelligence and machine learning into the clinical workflow. These advances in non-invasive cardiac imaging have guided patient management and improved clinical outcomes. The technological developments of the past 20 years have also given rise to new imaging subspecialties and increased the demand for dedicated cardiac imagers who are cross-trained in multiple modalities. This state-of-the-art review summarizes the evolution of multimodality cardiac imaging in the 21st century and highlights opportunities for future innovation.

INTRODUCTION

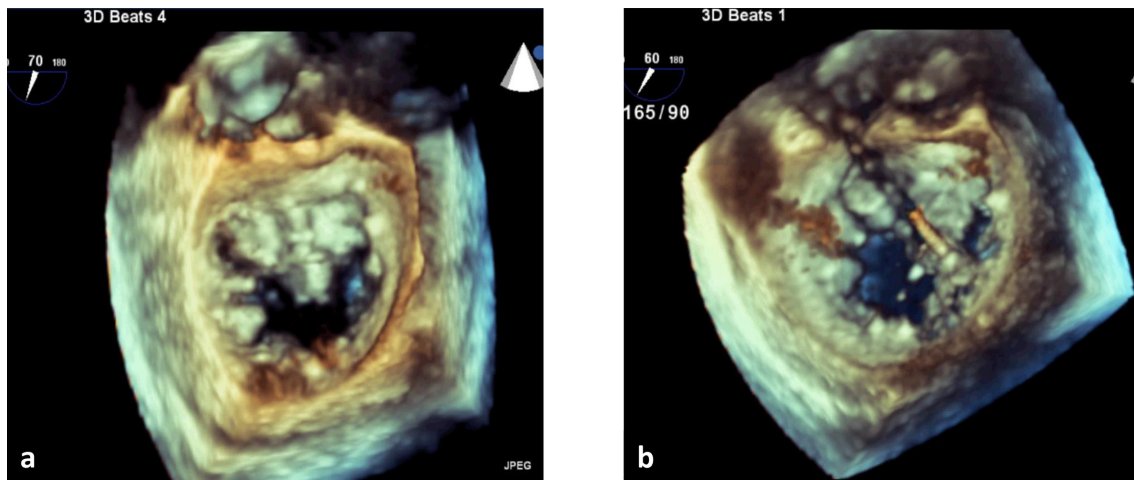
Multimodality imaging, including echocardiography, cardiac computed tomography (CCT), cardiac magnetic resonance (CMR) and nuclear cardiology [single-photon emission computed tomography (SPECT) and positron emission tomography (PET)], has fundamentally advanced the understanding and treatment of cardiovascular disease in the 21st century. These advances have impacted the non-invasive evaluation of coronary artery disease, structural heart disease, arrhythmias, and heart failure, as well as guided clinical management and improved patient outcomes. Several special populations are now better served as a result of the advancements in non-invasive imaging, such as patients with cardiac amyloidosis, women with coronary microvascular dysfunction, and high-risk individuals with severe valvular heart disease. Additionally, the use of artificial intelligence and machine learning applications in cardiac imaging has identified previously unrecognized patterns of disease, refined the assessment of cardiovascular risk, and influenced clinical care in an actionable and more personalized way than ever before. The tremendous technological revolution in the last two decades has also given

rise to new imaging subspecialties, such as interventional echocardiography, and increased the demand for dedicated cardiac imagers who are cross-trained in multiple modalities. This state-of-the-art review summarizes the evolution of multimodality cardiac imaging in the 21st century and highlights the opportunities for future innovation.

ECHOCARDIOGRAPHY

Echocardiography is often the first-line evaluation for the assessment of cardiac structure and function given the high temporal and spatial resolution, portability, cost-effectiveness and lack of ionizing radiation. In the last two decades, echocardiography has seen the rise of three-dimensional (3D) echocardiography for the quantitative evaluation of left ventricular (LV) function and structural heart disease.¹ Compared to two-dimensional (2D) echocardiography, real-time full volume 3D echocardiography does not use geometric assumptions about LV geometry making it a more accurate and reproducible means of measuring LV volumes and systolic function and has good correlation with CMR.^{2,3} Additionally, LV volumes and ejection fraction (EF) derived from 3D echocardiography have been shown to have a stronger association

Figure 1. Three-dimensional transesophageal echocardiography performed during percutaneous mitral valve repair for severe mitral regurgitation secondary to mitral valve prolapse. (a) Mitral valve (surgeon's view) with myxomatous mitral valve, prolapse of the anterior mitral valve leaflet and large regurgitant orifice. (b) Catheter deploying mitral valve clip between anterior and posterior mitral valve leaflets.

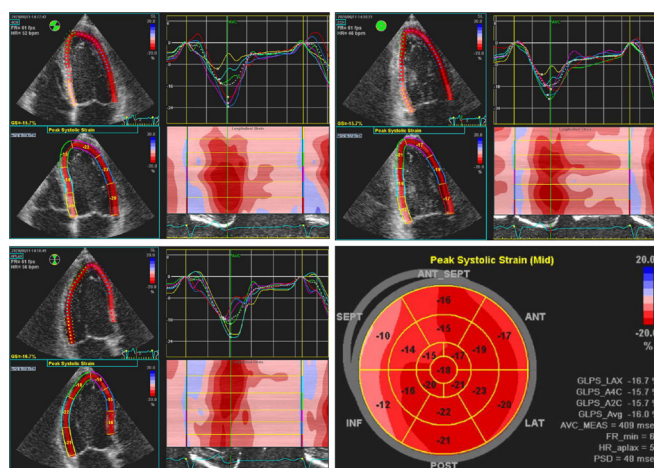


with clinical outcomes than those derived from 2D echocardiography.⁴ 3D echocardiography is also ideally suited to assess valve function given the nonplanar anatomy and spatial alterations resulting from valvular heart disease. Three-dimensional echocardiography has provided significant mechanistic insight about functional and ischemic mitral regurgitation by demonstrating derangements in the complex relationship of the mitral valve leaflets, chordal attachments, papillary muscles and the LV myocardium.¹ Interventional echocardiography, a new subspecialty in cardiac imaging, frequently employs 3D transesophageal echocardiography for the real-time assessment of valve anatomy, which is integral to guiding percutaneous valvular interventions,

particularly transcatheter aortic valve replacement (TAVR),^{5,6} mitral valve clip repair,^{7,8} and most recently transcatheter mitral and tricuspid valve implantation (Figure 1).⁹⁻¹¹

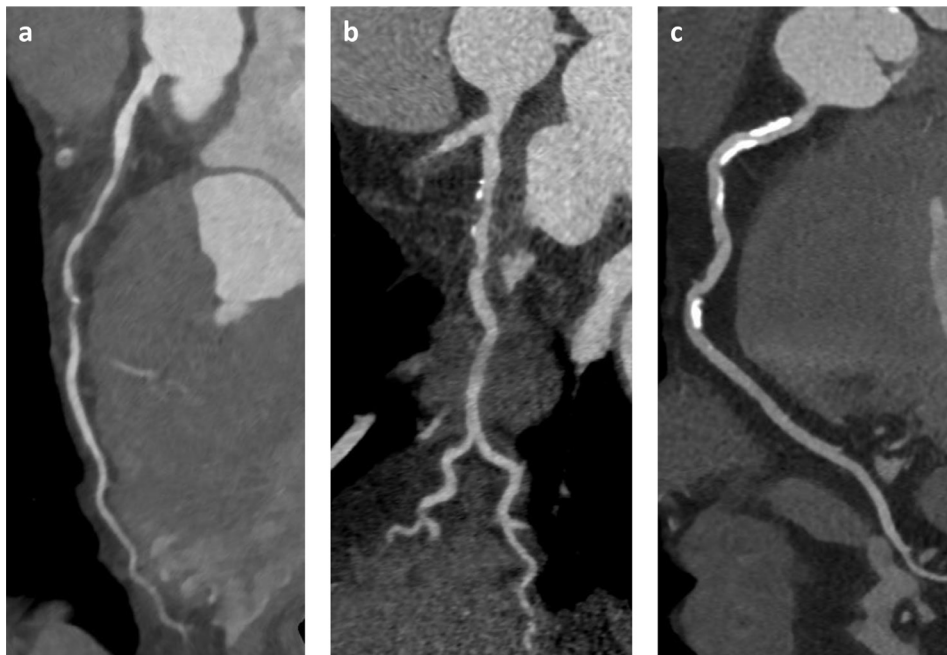
Figure 2. Regional strain analysis with speckle-tracking echocardiography in the apical 4-chamber, 2-chamber, and 3-chamber views demonstrates left ventricular dyssynchrony in a patient with LBBB. The characteristic LBBB contraction pattern on strain imaging includes early terminated shortening in the septal wall, early (pre-stretch) contraction in the lateral wall, and late lateral peak contraction. LBBB, left bundle branch block.

Advances in image-based analysis of local myocardial dynamics, including Doppler tissue imaging (DTI) and speckle-tracking echocardiography (STE), have allowed for the quantitative assessment of subclinical myocardial dysfunction.¹² Myocardial deformation, measured by strain and strain rate using DTI and STE, has demonstrated that early decreases in radial and longitudinal strain and strain rate among patients treated with cardiotoxic oncologic treatments, such as anthracyclines, taxanes and trastuzumab, precede decreases in EF and are therefore capable of detecting prognostically important subclinical LV dysfunction.¹³ Similarly, global longitudinal strain (GLS) on STE has been useful in risk stratifying patients with asymptomatic severe aortic stenosis (AS) and preserved EF, such that impaired LV GLS has been associated with a higher risk of developing symptoms and needing aortic valve intervention as compared to patients with normal LV GLS.¹⁴ Detection of LV dyssynchrony with DTI or STE has been associated with long-term survival and is used to optimize cardiac resynchronization therapy in patients with advanced systolic heart failure (Figure 2).^{15,16} Regional differences in myocardial dynamics as assessed by STE has been insightful for the detection of cardiac involvement in systemic disease, such as amyloidosis, which exhibits a characteristic apical-sparing pattern.¹⁷ Furthermore, the use of STE for strain and strain rate analysis to quantitate myocardial contraction and relaxation during stress echocardiography is an active area of clinical investigation.¹⁸



Finally, cardiac point-of-care ultrasound (POCUS), with its compact size, exceptional portability and ease of use, is increasingly utilized in settings such as emergency rooms and critical care settings to provide rapid bedside diagnosis of cardiovascular pathology.¹⁹ This technology has also been successfully deployed to improve access to care in remote regions with limited

Figure 3. Coronary artery disease on CCTA reveals severity of luminal stenosis and composition of atherosclerotic plaque in the vessel wall: (a) non-calcified plaque; (b) mixed plaque with calcified and non-calcified components; (c) densely calcified plaque. CCTA, cardiac CT angiography.



resources, as well as a means to decrease transmission while evaluating cardiac complications during the recent COVID-19 pandemic.²⁰

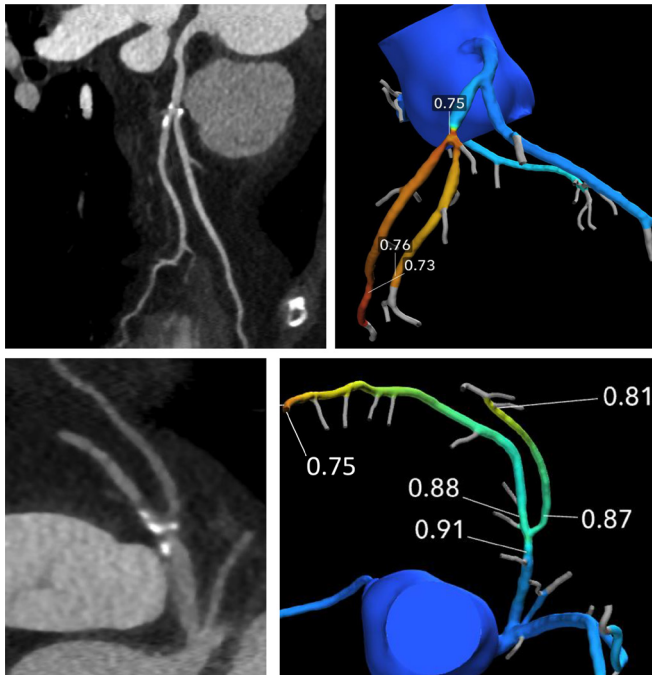
CARDIAC COMPUTED TOMOGRAPHY

The use of CCT in clinical practice has dramatically increased in the 21st century. The introduction of multidetector computed tomography (MDCT) in 1998 was an evolutionary leap for anatomic imaging and led to the exponential growth in MDCT technology in the subsequent decade. The current minimum standard for cardiac CT angiography (CCTA) is 64-slice MDCT, which was first available in 2005. By 2008, advancements in CT technology had resulted in 256- and 320-slice MDCT scanners capable of capturing the whole heart in one to two rotations, which significantly decreased both acquisition time and image artifact.²¹ Furthermore, the high spatial and temporal resolution of CCTA is ideally suited for the evaluation of coronary artery disease (CAD). Similar to cardiac catheterization, CCTA provides an anatomic assessment of CAD and the degree of luminal stenosis, but unlike invasive angiography, CCTA also reveals the burden and composition of plaque within the vessel wall (Figure 3). These capabilities make CCTA highly sensitive (sensitivity 95–99%) for the identification of both obstructive and non-obstructive CAD and affords a high negative predictive value (NPV 97–99%) for the exclusion of CAD.^{22,23} This non-invasive insight about CAD burden can be effectively used to manage and prognosticate patients. For example, non-obstructive CAD, which would not elicit ischemic changes on functional imaging, but is readily identified by CCTA, has been associated with increased adverse cardiac events, particularly among women, even in the absence of obstructive CAD.^{24–26} Additionally, the demonstration of non-obstructive disease

would effectively reclassify these patients as needing secondary, rather than primary CAD prevention, which has implications for medical management, such as statin therapy, and is currently being studied in the WARRIOR trial (<https://clinicaltrials.gov/ct2/show/NCT03417388>). CCTA also permits the quantification and characterization of atherosclerotic plaque. High-risk plaque characteristics such as positive remodeling, spotty calcification, and low attenuation (<30 HU) plaque have been shown to identify vulnerable coronary lesions that are associated with an increased risk of acute coronary syndrome (ACS).^{27–29} Currently, research is being conducted on novel analytical techniques to facilitate the detection and quantification of pericoronary inflammation and atherosclerotic plaque activity on CCTA, which may serve to further improve cardiac risk prediction and optimize clinical outcomes in patients with CAD.³⁰

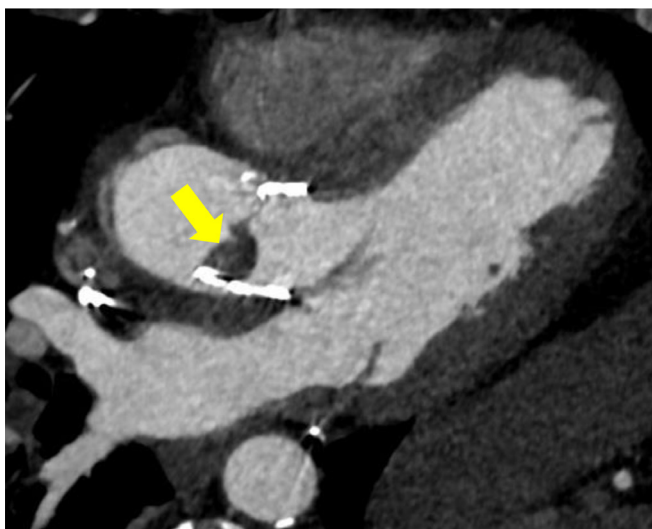
Compared to 20 years ago, improvements in scanner technology, acquisition techniques, and iterative reconstruction software have collectively and significantly minimized radiation exposure during CCTA.³¹ Furthermore, although CCTA was only initially capable of yielding an anatomic assessment of CAD, the application of computational fluid dynamics and machine learning to CCTA data sets provides a non-invasive estimation of fractional flow reserve (CT-FFR) and identification of flow-limiting, hemodynamically significant lesions (Figure 4).³² CT-FFR assesses resistance and flow along the coronary arteries to identify lesion-specific ischemia and has been validated in multiple trials with good correlation with invasive FFR.^{33–35} The integration of CT-FFR with CCTA allows for an anatomical and functional assessment of CAD with a single test and results in higher diagnostic accuracy and increased specificity for classification of flow-limiting coronary stenosis than CCTA alone, which is

Figure 4. The degree of stenosis of the left anterior descending artery at the take-off of the first diagonal branch appears similar in the curved planar reformation CCTA images in these two patients. However, CT-FFR analysis demonstrates that the atherosclerotic plaque in the upper row is a flow-limiting stenosis with a CT-FFR value of less than 0.8 after the lesion, while the plaque in the bottom row does not result in a hemodynamically-significant obstruction of coronary blood flow on CT-FFR. CT-FFR, CT-fractional flow reserve; CCTA, cardiac CT angiography.



important for guiding patient management.^{34,35} The combined use of CCTA and CT-FFR has been shown to act as an effective gatekeeper to the catheterization laboratory by reducing the

Figure 5. CCTA demonstrating thrombus (arrow) on aortic valve leaflet after TAVR. CCTA, cardiac CT angiography; TAVR, transcatheter aortic valve replacement.



need for invasive evaluation of patients without lesion-specific ischemia.³⁶ Additionally, CT-FFR has prognostic implications, such that patients with CAD and normal CT-FFR (>0.80) have lower rates of adverse cardiac events than those with abnormal CT-FFR values of ≤ 0.80 .³⁷ Furthermore, when adverse plaque characteristics on CCTA are integrated with CT-FFR results, the prognostic stratification is superior to either component alone.³⁸

Myocardial CT perfusion (CTP) with pharmacologic stress provides a combined assessment of cardiac anatomy and physiology. Similar to CMR, CTP imaging performed immediately after contrast administration can reveal hypoenhancement corresponding to perfusion defects while delayed imaging, acquired 5–10 min after contrast administration, may show regional hyperenhancement indicating areas of myocardial necrosis or scar.³⁹ Compared to CCTA alone, CTP increases the diagnostic accuracy for the detection or exclusion of ischemia.⁴⁰ CTP performs comparably with CMR and PET and outperforms SPECT for the evaluation of hemodynamically significant CAD.⁴¹ Despite these advantages however, operational challenges, variation in quantitative values, scanner availability and the requisite expertise have limited the widespread adoption of CTP in routine clinical practice.

Cardiac CT has also played an integral role in the evaluation and treatment of structural heart disease. The isotropic resolution of cardiac CT allows image manipulation in any plane or orientation without distortion, yielding a true 3D imaging assessment of the heart and surrounding anatomy. This robust capability has led to the increased utilization of cardiac CT to guide percutaneous interventions for valvular heart disease, congenital heart disease and atrial fibrillation. In patients with severe aortic stenosis, cardiac CT has significantly improved the pre-procedural planning process prior to TAVR and provided unique insight about post-TAVR complications, such as acute and subacute thrombosis and infection (Figure 5).^{42–45} More recently, cardiac CT has also been employed in patients with mitral and tricuspid valve disease prior to transcatheter interventions.⁴⁶ Cardiac CT provides highly detailed information about cardiac anatomy and dimensions to optimize device sizing, as well as reveal anatomic considerations that can determine vascular access routes and reduce the risk of procedural complications.^{47,48} In patients with atrial fibrillation, cardiac CT is used to delineate the pulmonary vein anatomy prior to ablation, assess for intracardiac thrombus, and visualize left atrial appendage morphology. Pre-procedural CT measurements are critical to the successful deployment of appendage exclusion devices among patients with contraindications to long-term anticoagulation.⁴⁹ Finally, cardiac CT is also showing promise for the detection of cardiac allograft vasculopathy after heart transplantation and identification of cardio-mechanical complications among patients with suspected left ventricular assist device (LVAD) malfunction.^{50,51}

CARDIAC MAGNETIC RESONANCE IMAGING

CMR imaging is a highly versatile modality for the evaluation of cardiac pathology. Historically, CMR has been reserved for the evaluation of complex congenital heart disease, cardiac tumors and pericardial disease.^{52–54} However, over time CMR has been

shown to be superior to other non-invasive modalities for the assessment of biventricular morphology and function and is considered the reference standard for quantitation of ventricular volumes.^{2,55} Additionally, CMR is unique for its tissue characterization capabilities and the identification of myocardial scar, fibrosis, edema and inflammation. As a result, the leading indications for a CMR evaluation include: 1. Investigation of myocarditis and cardiomyopathies; 2. evaluation of CAD and ischemia; and 3. assessment of myocardial viability.⁵⁶

CMR imaging is an unparalleled diagnostic tool in the evaluation of cardiomyopathies and myocarditis. The presence and extent of late gadolinium enhancement (LGE) imaging serves as a critical sequence in the differentiation of ischemic vs non-ischemic heart disease.⁵⁷ Non-ischemic cardiomyopathies demonstrate

distinct LGE patterns, such as LGE in a non-coronary distribution involving the mid-myocardium, epicardium, and or diffuse subendocardial locations. In addition to LGE imaging, advances in T1, T2, and T2* imaging and mapping, which are capable of detecting infiltrative disorders, inflammation and edema, also provide insight into non-ischemic etiologies. For instance, myocardial T2 imaging correlates with myocardial free water content, which can be particularly valuable in identifying patients with acute myocarditis (Figure 6).^{58,59} The sensitivity of CMR for the detection of acute myocarditis has also been increased by T1 and T2 parametric maps that outperform the original Lake Louise Criteria, which predominantly rely on LGE imaging.⁶⁰ In recent years, T1 mapping has also gained clinical application for the detection of cardiac amyloidosis.^{61,62} While LGE is useful in the diagnosis of cardiac amyloid, the characteristic pattern of

Figure 6. Acute myocarditis and follow-up evaluation by CMR imaging. (a) LGE imaging demonstrates mid-myocardial and epicardial enhancement involving the lateral and inferolateral left ventricular wall (arrows), in a pattern most characteristic of myocarditis. (b) T_2 weighted imaging reveals hyperintensity in the lateral LV wall (arrows), indicating edema and suggesting active myocardial inflammation. Follow-up CMR imaging was performed 1.5 years later: (c) LGE imaging demonstrates myocardial scarring, as indicated by epicardial and mid-myocardial enhancement in the lateral and inferolateral walls (arrows). (d) T_2 weighted imaging is normal, which indicates that the previously seen myocardial edema has resolved, suggesting the absence of active inflammation. CMR, cardiac magnetic resonance; LGE, late gadolinium enhancement; LV, left ventricular.

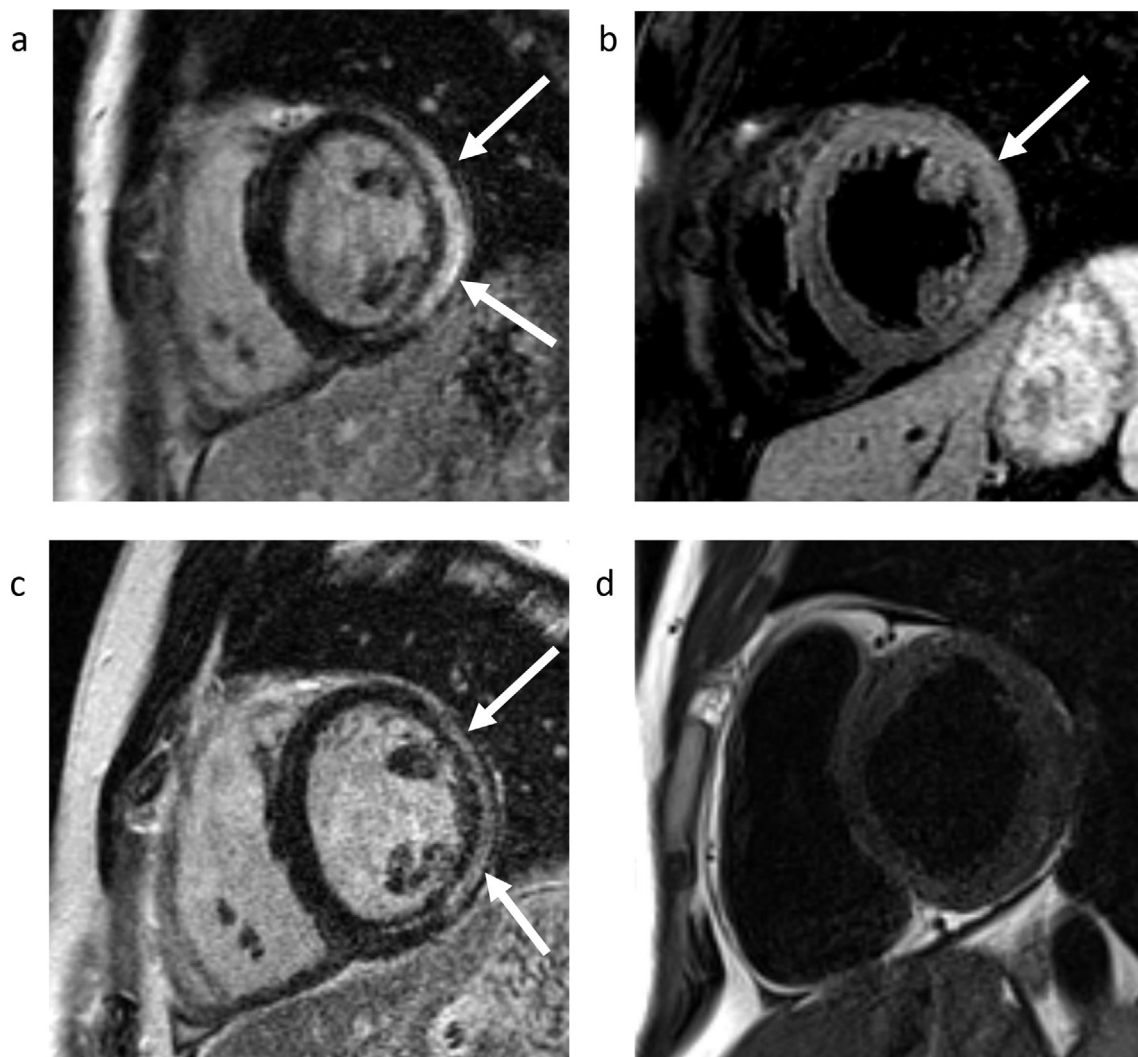
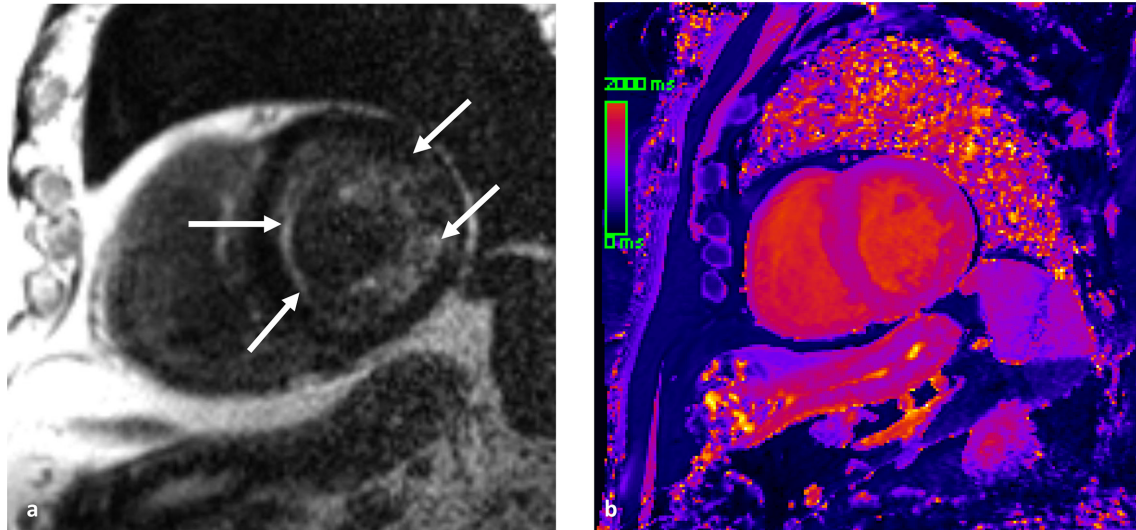


Figure 7. Cardiac amyloidosis diagnosed by CMR imaging. (a) LGE imaging demonstrates diffuse subendocardial enhancement, as well as patchy mid-myocardial enhancement (arrows). The diffuse subendocardial pattern of enhancement, in conjunction with the black blood pool, is characteristic for cardiac amyloidosis. (b) Non-contrast T1 mapping demonstrates heterogenous high T1 values in the myocardium. The measured average T1 time was 1407 ms (normal reference = 950 ± 21 ms). CMR, cardiac magnetic resonance; LGE, late gadolinium enhancement.

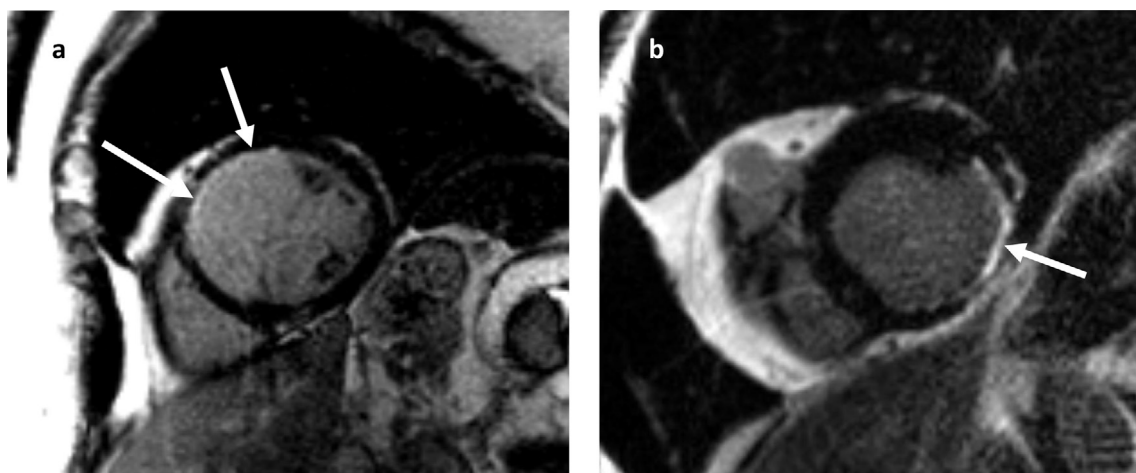


diffuse subendocardial enhancement may not always be present or may occur late in the disease process. Whereas non-contrast T1 mapping can be valuable for identifying amyloid infiltration at an early stage and also has benefit in patients with renal failure, in whom gadolinium may be contraindicated. Quantitative T1 mapping yields significantly higher T1 times in individuals with cardiac amyloid compared with normal controls (Figure 7). With a 1.5 T CMR, a non-contrast myocardial T1 threshold of 1020 ms has greater than 90% accuracy for cardiac involvement in patients with amyloid.⁶¹ These quantitative mapping techniques have also been shown to have application in the diagnosis of heart transplant rejection; hypertrophic cardiomyopathy; myocardial iron

accumulation in hemochromatosis, sickle cell disease and beta-thalassemia major; and cardiac involvement in systemic diseases, such as sarcoidosis and Fabry disease.⁶³⁻⁶⁵

LGE in a coronary artery distribution is the hallmark feature of myocardial infarction in CAD (Figure 8). With prolonged coronary artery occlusion, a subendocardial infarct may progress in a transmural fashion, thereby exhibiting transmural enhancement. In the setting of CAD, LGE burden can provide important prognostic information prior to revascularization therapy. The turn-of-the-century landmark publication by Kim et al, revealed that the extent of transmural LGE is inversely proportional to the

Figure 8. Late gadolinium enhancement in a coronary artery distribution is the hallmark feature of myocardial infarction. (a) Subendocardial infarct in the LAD territory, spanning less than 25% myocardial wall thickness (arrows). (b) Myocardial infarction of the left circumflex artery. LGE CMR imaging in the short axis plane demonstrates myocardial wall thinning and transmural enhancement in the inferolateral wall of the left ventricle (arrow). CMR, cardiac magnetic resonance; LAD, left anterior descending; LGE, late gadolinium enhancement.



likelihood of functional myocardial recovery following revascularization therapy.⁶⁶ These findings have been validated in a number of subsequent studies, which have shown that myocardium with subendocardial infarct (LGE spanning $\leq 25\%$ wall thickness) has a higher association with functional recovery after revascularization than myocardium demonstrating transmural infarct (LGE spanning $\geq 75\%$ wall thickness), with the latter group experiencing almost no improvement in contractility despite revascularization.^{67,68} Hence, LGE provides a valuable non-invasive method of stratifying individuals with myocardial infarct in whom revascularization may offer potential benefit.

Stress CMR has excellent diagnostic and prognostic value.⁶⁹ Although stress CMR accounts for less than 5% of stress imaging, CMR has been shown to be more sensitive than other perfusion modalities for the detection of significant CAD and a CMR-guided management strategy for ischemia-inducing CAD has been associated with a lower incidence of coronary revascularization than an invasive FFR-guided strategy with no difference in major adverse events after 1 year.^{70,71} Furthermore, CMR perfusion can provide insight on alternative etiologies of chest pain. Due to the high spatial and temporal resolution, CMR perfusion can identify microvascular disease, which may manifest as diffuse subendocardial hypoperfusion on first-pass perfusion CMR.⁷² In patients with ACS who are found to have myocardial infarction with non-obstructive coronary arteries (MINOCA), early CMR can narrow the differential diagnosis in 84% of cases, thus distinguishing between myocarditis, myocardial infarction (type II or spontaneous thrombolysis), and Takotsubo cardiomyopathy.⁷³

Despite all of these capabilities and the lack of ionizing radiation, the main limitations for greater utilization of CMR remain the need for highly trained experts for acquisition and interpretation, the requisite equipment, and the long exam duration. The presence of an implantable cardiac device, such as a pacemaker or internal defibrillator, was also a contraindication to CMR until recently. Newer devices have been developed to be MRI compatible, but still require reprogramming into an MRI safe mode and artifacts that affect LGE and functional evaluations may persist.⁷⁴ Finally, artificial intelligence applications for CMR that minimize scan times, improve reproducibility through automated segmentation, and identify scar on non-contrast images for patients with contraindications to gadolinium contrast may make implementation of this highly versatile imaging modality more widespread.^{75,76}

NUCLEAR CARDIOLOGY

Nuclear cardiology is the most frequently used functional imaging test and as a result has a wealth of evidence related to diagnosis and long-term prognosis. Radionuclide myocardial perfusion imaging is currently dominated by SPECT, which evaluates the relative distribution of coronary blood flow in the myocardium (Figure 9). The sensitivity and specificity of SPECT for the diagnosis of CAD is 87–79 and 73–75%, respectively, varying by the radionuclide and stress modality employed.⁷⁷ Since its inception in 1980, SPECT imaging has evolved considerably. Recent developments have included cadmium zinc telluride

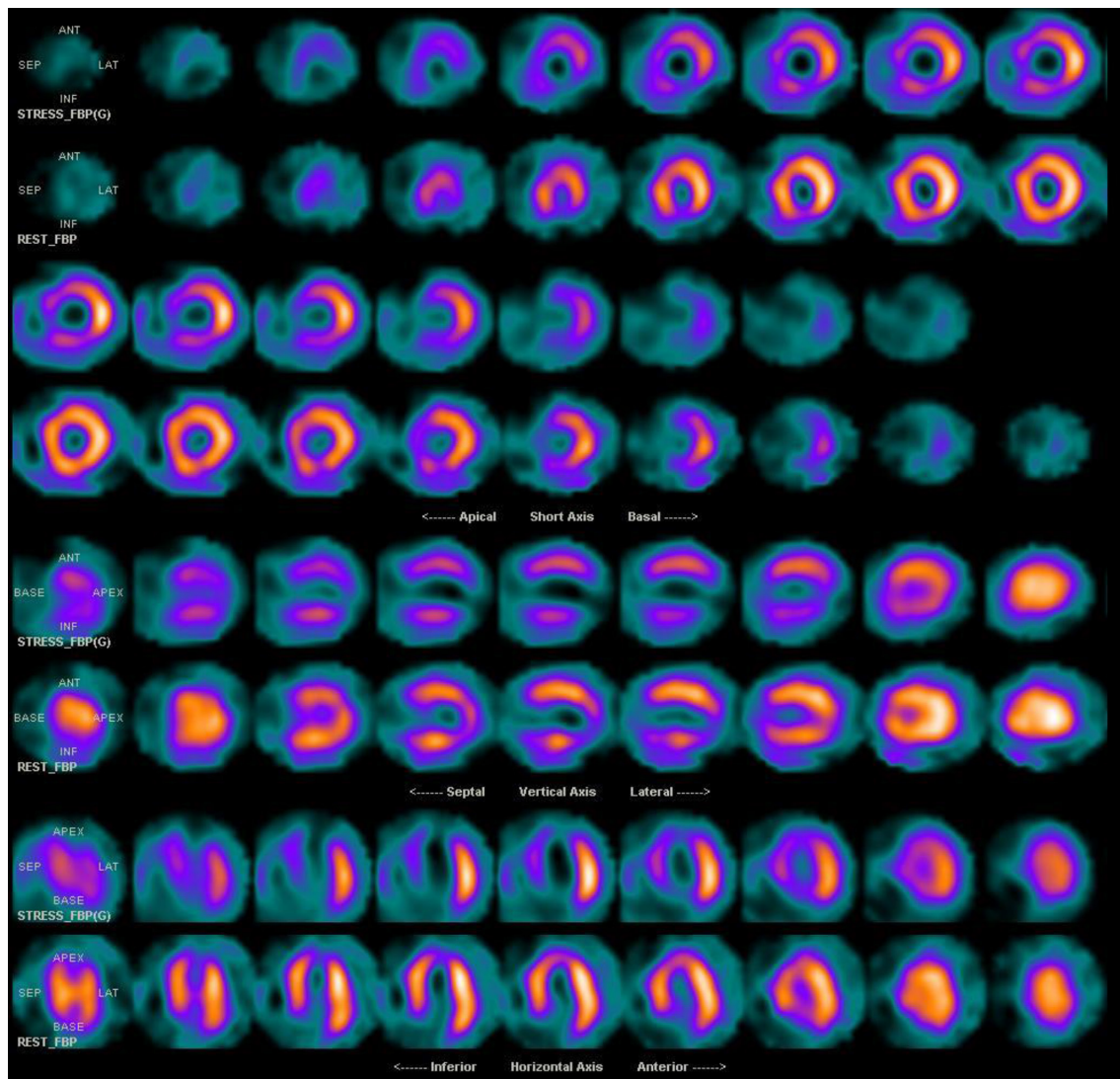
(CZT) detectors, γ cameras, iterative reconstruction and $\frac{1}{2}$ dose or $\frac{1}{2}$ time software that decrease radiation exposure, expedite image acquisition, and improve image resolution.^{78–80} However, despite these technological advances, SPECT remains limited by the qualitative, or at best semi-quantitative, methods for identifying myocardial ischemia. In patients with multivessel CAD, SPECT may underestimate the true extent of disease since the likelihood of detection is highest with severe lesions but lower with milder stenosis. Additionally, because of the reliance upon relative differences in counts on SPECT, patients with a balanced reduction in myocardial blood flow may have a paradoxical normal or near-normal scan despite the presence of extensive high-risk CAD.

In contrast to SPECT, PET myocardial perfusion imaging is capable of true quantification of myocardial perfusion both globally and regionally. Quantifying regional perfusion is useful in patients with diffuse, multivessel CAD where the relative assessment of myocardial perfusion by SPECT may fail to reveal underlying disease.⁸¹ The sensitivity of PET for the diagnosis of CAD is 90–93% with a specificity of 89–92%.⁸² PET is also capable of generating absolute measurements of myocardial blood flow. This capability is not only useful for the detection of epicardial CAD, but quantitative PET measurements of blood flow are playing an increasingly important role in the evaluation and management of patients with suspected coronary microvascular dysfunction. Specifically, the inability to increase stress myocardial blood flow > 2.0 to $2.4 \text{ mL} \times \text{min}^{-1} \times \text{g}^{-1}$ in the absence of obstructive epicardial disease is indicative of coronary microvascular disease.⁸³ Additionally, PET has been applied to assess coronary endothelial function in response to pharmacologic therapies (*i.e.* statin), toxins (*i.e.* tobacco), and disease states, such as diabetes mellitus, obesity, and hypertension.^{82,84} PET is also capable of assessing myocardial viability using the glucose analogue and metabolic tracer fludeoxyglucose, FDG (Figure 10). Although the utility of myocardial viability in guiding clinical care remains uncertain, a pooled analysis demonstrated a weighted mean sensitivity and specificity of 92 and 63%, respectively, for regional functional recovery.⁸⁵

Finally, cardiovascular molecular imaging is a rapidly evolving discipline that aims to visualize specific molecular targets and pathways to provide insight about morphology and pathophysiology. Examples include neuronal imaging to identify patients at risk for ventricular arrhythmia, imaging compounds that target vulnerable plaque prior to ACS, and identifying molecular imaging markers that reflect adverse LV remodeling before the development of overt heart failure.^{86–88} Despite the many advantages of PET, its widespread use in clinical care has been limited by the relatively high costs, technical complexities, and requisite professional expertise that was previously restricted to specialized cardiac centers. However, the increasing evidence base combined with the ability to perform myocardial blood flow imaging has led to considerable growth and utilization of PET in clinical practice.

In addition to the detection of CAD, myocardial perfusion imaging has also been employed in the detection of cardiac

Figure 9. Exercise stress (top) and rest (bottom) myocardial perfusion imaging study with SPECT. Reversible changes in the septum, anterior, inferior and apical segments compatible with ischemia. Transient ischemic dilatation is noted with TID index of 1.3. Cardiac catheterization demonstrated proximal 90% LAD stenosis and 90% mid-RCA stenosis. LAD, left anterior descending; RCA, right coronary artery; SPECT, single-photon emission computed tomography; TID, transient ischemic dilation.

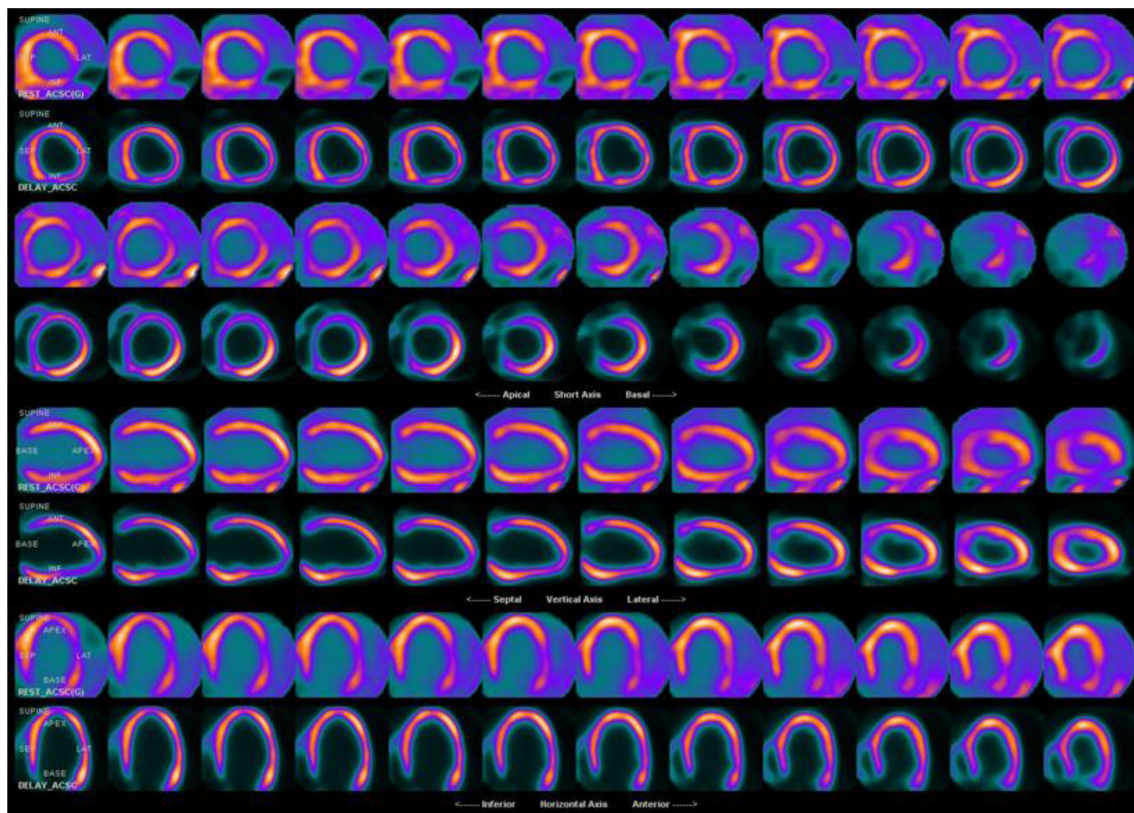


manifestations of systemic disease. Transthyretin cardiac amyloidosis (also known as ATTR cardiac amyloidosis) is an increasingly recognized cause of heart failure with preserved ejection fraction (HFpEF). With newly targeted therapies available for the treatment of ATTR cardiac amyloidosis, it is critical to have a non-invasive imaging test to identify and differentiate among HFpEF patients with cardiac amyloidosis. Planar and SPECT imaging using Tc 99m PYP, Tc 99m DPD, or Tc 99m HMDP are useful for the detection of ATTR amyloid fibrils in the myocardium (Figure 11).⁸⁹ A recent multicenter study, confirmed that Tc 99m PYP cardiac imaging has a sensitivity of 88% and specificity of 88% for the differentiation of ATTR cardiac amyloidosis from light-chain-related amyloidosis and nonamyloid HFpEF.⁹⁰ Furthermore, a heart to contralateral (H/CL) ratio of ≥ 1.6 was associated with worse survival among patients with ATTR cardiac amyloidosis.

HYBRID AND FUSION IMAGING

There is a complex relationship between coronary stenosis and myocardial ischemia. A number of landmark studies in the last two decades have consistently demonstrated that the angiographic severity of coronary lesions is a poor predictor of hemodynamic relevance.^{91–93} Importantly, stenosis alone is insufficient to identify flow-limiting lesions among patients with stable CAD. A comparison study of CCTA and SPECT showed that only 32% of obstructive coronary lesions, defined as $\geq 50\%$ stenosis, were associated with perfusion defects on SPECT.⁹⁴ Similarly, the FAME trial demonstrated that stenoses of 50–70% on coronary angiography can be functionally significant according to a FFR of ≤ 0.8 , while coronary lesions with $>70\%$ stenosis may not be ischemia-inducing based on a FFR value of >0.8 .⁹⁵ Thus, in the last two decades there has been a paradigm shift in the treatment of CAD with emphasis on the importance of myocardial ischemia to guide clinical management.

Figure 10. PET assessment of myocardial viability in patient with triple vessel obstructive coronary artery disease and reduced ejection fraction. Top rows: N-13 ammonia at rest show diminished perfusion in the lateral wall. Lower rows: F-18 FDG reveal preserved metabolic FDG uptake in the corresponding lateral segments, as well as the remaining myocardium, which signifies the presence of viable myocardium. FDG, fludeoxyglucose; PET, positron emission tomography.



Hybrid cardiac imaging, which combines morphologic and anatomic results with functional evaluations of myocardial perfusion, has the ability to detect the presence of coronary lesions and their hemodynamic significance and therefore has superior diagnostic performance compared with anatomic or functional modalities alone. A hybrid approach utilizing SPECT or PET and cardiac CT has allowed for the simultaneous identification of flow-limiting coronary stenosis and ischemia quantification in a single assessment, which may be useful for informing clinical management.⁹⁶ Furthermore, when nuclear myocardial perfusion imaging is used in conjunction with CT, the hybrid imaging approach minimizes attenuation artifact and dramatically improves diagnostic and prognostic robustness.^{97,98} Image coregistration and fusion of 3D information about myocardial territories and their coronary supply can accurately identify the culprit ischemic lesion in multivessel CAD, which is important since there is evidence that perfusion defects do not correspond to the expected coronary distribution in >50% of cases.^{99,100} Hybrid imaging with PET and CT or CMR has also been utilized in the evaluation of cardiac sarcoidosis, which permits the simultaneous evaluation of myocardial inflammation with LGE sequences and correlative metabolic activity on PET images that aids in the differentiation of inflammation and scar (Figure 12).¹⁰¹

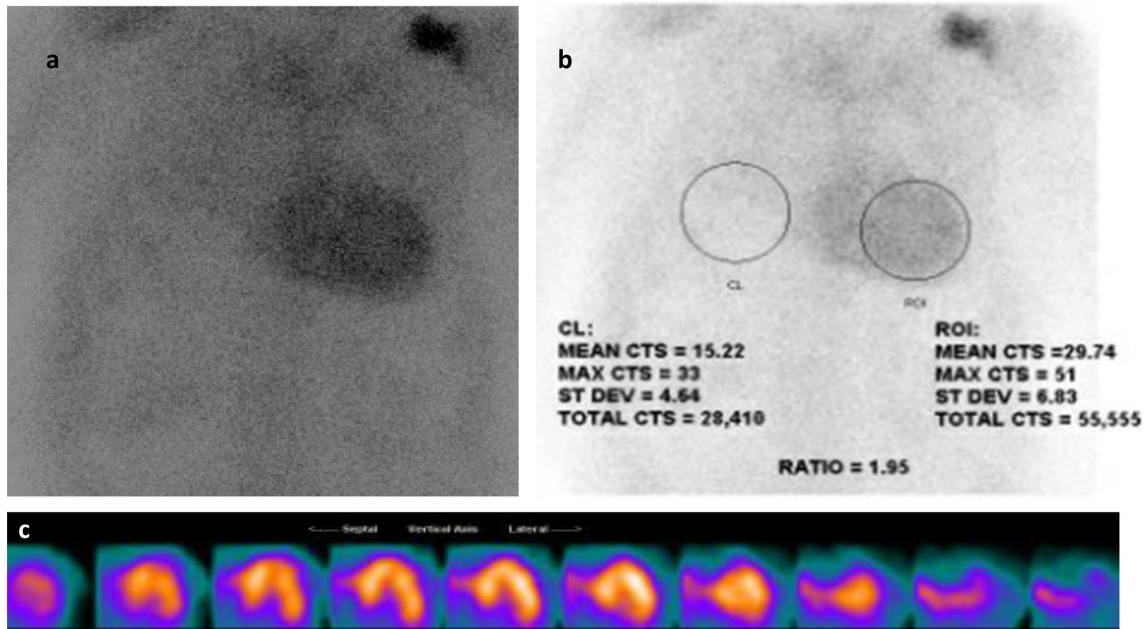
The 21st century has also seen the rise of fusion imaging, whereby images obtained separately with different modalities are fused

into a composite image. Harmonizing two modalities provides a better understanding of the 3D relationship of anatomy and devices, increases procedural efficiency, and improves clinical outcomes.¹⁰² The overlay of TEE or CT images and fluoroscopy have significantly aided the successful deployment of percutaneous interventions for congenital and structural heart disease.^{103,104} CCTA or CMR images superimposed on electrical mapping systems in the electrophysiology laboratory have improved the success of radiofrequency ablation for atrial fibrillation and the placement of LV leads to decrease dyssynchrony with cardiac resynchronization therapy.^{102,105}

ARTIFICIAL INTELLIGENCE AND MACHINE LEARNING IN CARDIAC IMAGING

The most recent advancement in cardiac imaging in the 21st century is the application of artificial intelligence (AI) for the integration of cardiovascular imaging and “big data,” which is likely to result in new discoveries, better characterize disease and uniquely personalize therapy. The increasing use of AI may also reduce cost and enhance value during image acquisition, interpretation, reporting, and decision management. Machine learning (ML) is a subset of AI wherein information is acquired autonomously by extracting patterns from large databases giving AI the ability to learn and deep learning is a means of informing associations based on previous experience, effectively training the process so that the probability of correct classification increases.^{106,107} Uses of AI and ML that have been applied

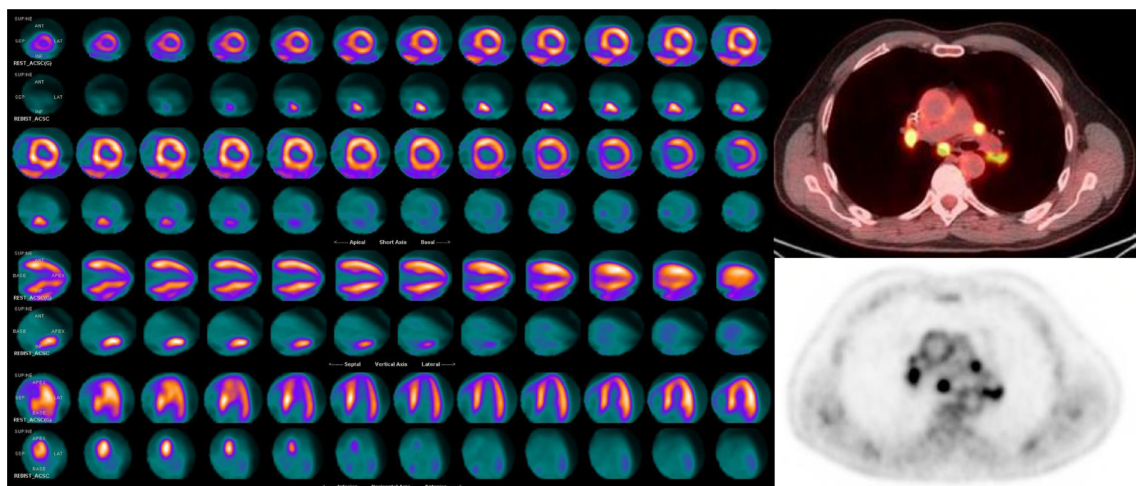
Figure 11. Tc-99m Pyrophosphate planar and SPECT imaging for cardiac amyloid. (a) Increased activity is seen over the heart on planar imaging. (b) Quantitative analysis of H/CL ratio is 1.95 (Negative <1.5), strongly suggestive of TTR amyloidosis. C. SPECT imaging confirms intense diffuse uptake in the left ventricular myocardium and to a lesser degree in the visible aspect of the right ventricle. Fine needle aspiration biopsy of the abdominal fat was positive for extracellular amyloid deposition. H/CL, heart-to-contralateral lung; SPECT, single photon emission tomography.



to cardiac imaging include automating quantitative measuring, generating problem notifications and providing diagnostic support tools. Examples of these applications have included: (1) the fully automated LV segmentation and volume measurement on CMR^{75,108}; (2) identification of three different echocardiographic phenotypes among patients with diabetes mellitus Type 2 and the associated distinct clinical profiles¹⁰⁹; and (3) automated analysis of the myocardium on CCTA to identify

hemodynamically significant coronary stenosis.¹¹⁰ Integrating clinical data and imaging measures has also improved prediction of prognostic outcomes. ML of combined clinical and CCTA data was more predictive of mortality than either clinical or CCTA metrics alone.¹¹¹ Similarly, compared to automated perfusion quantification alone, ML had higher predictive accuracy for major adverse cardiac events using a combination of clinical information and SPECT perfusion assessments.¹¹² Finally,

Figure 12. Cardiac PET: N-13 ammonia rest images (top rows) demonstrate a perfusion defect in the basal and mid inferoseptum, extending from the epicardium to the subendocardium. F-18 FDG images (lower rows) demonstrate focal hypermetabolism in the areas of perfusion defect, consistent with active inflammation in this area. Hybrid CT and F-18 FDG images of the chest show hypermetabolic hilar and mediastinal lymphadenopathy, compatible with active chest sarcoidosis. The integration of the chest and cardiac findings are consistent with sarcoidosis. FDG, fluorodeoxyglucose; PET, positron emission tomography.



research using radiomics, the process of obtaining quantitative metrics from images to create big-data data sets, such as where each coronary lesion is characterized by hundreds of different parameters, may further improve cardiac risk prediction and optimize clinical outcomes in patients with CAD.³⁰ Future development of AI with large imaging registries and repositories will increase diagnostic and prognostic performance, as well as individualize the value of cardiac imaging in clinical medicine.

CONCLUSIONS

The tremendous technological evolution achieved in non-invasive imaging techniques over the last two decades, including

echocardiography, CCT, CMR, and nuclear cardiology have provided clinicians with a large non-invasive armamentarium for the assessment of cardiac disease. Best practice, appropriate use, and clinical guidelines are constantly being updated with this evolving new data. The complementary information gained from different imaging modalities has yielded new insights about cardiovascular pathology and disease progression, guided and optimized patient care, and ultimately improved clinical outcomes. The cardiac imaging of today offers diagnostic, prognostic and risk stratification capabilities that were unimaginable only two decades ago.

REFERENCES

- Hung J, Lang R, Flachskampf F, Shernan SK, McCulloch ML, Adams DB, et al. 3D echocardiography: a review of the current status and future directions. *J Am Soc Echocardiogr* 2007; **20**: 213–33. doi: <https://doi.org/10.1016/j.echo.2007.01.010>
- Dorosz JL, Lezotte DC, Weitzenkamp DA, Allen LA, Salcedo EE. Performance of 3-dimensional echocardiography in measuring left ventricular volumes and ejection fraction: a systematic review and meta-analysis. *J Am Coll Cardiol* 2012; **59**: 1799–808. doi: <https://doi.org/10.1016/j.jacc.2012.01.037>
- Thavendiranathan P, Liu S, Verhaert D, Calleja A, Nitinunu A, Van Houten T, et al. Feasibility, accuracy, and reproducibility of real-time full-volume 3D transthoracic echocardiography to measure LV volumes and systolic function: a fully automated endocardial contouring algorithm in sinus rhythm and atrial fibrillation. *JACC Cardiovasc Imaging* 2012; **5**: 239–51. doi: <https://doi.org/10.1016/j.jcmg.2011.12.012>
- Stanton T, Jenkins C, Haluska BA, Marwick TH. Association of outcome with left ventricular parameters measured by two-dimensional and three-dimensional echocardiography in patients at high cardiovascular risk. *J Am Soc Echocardiogr* 2014; **27**: 65–73. doi: <https://doi.org/10.1016/j.echo.2013.09.012>
- Hahn RT, Nicoara A, Kapadia S, Svensson L, Martin R. Echocardiographic imaging for transcatheter aortic valve replacement. *J Am Soc Echocardiogr* 2018; **31**: 405–33. doi: <https://doi.org/10.1016/j.echo.2017.10.022>
- Hahn RT, Little SH, Monaghan MJ, Kodali SK, Williams M, Leon MB, et al. Recommendations for comprehensive intraprocedural echocardiographic imaging during TAVR. *JACC Cardiovasc Imaging* 2015; **8**: 261–87. doi: <https://doi.org/10.1016/j.jcmg.2014.12.014>
- Khalique OK, Hahn RT. Percutaneous mitral valve repair: multi-modality cardiac imaging for patient selection and Intra-Procedural guidance. *Front Cardiovasc Med* 2019; **6**: 142. doi: <https://doi.org/10.3389/fcvm.2019.00142>
- Bax JJ, Debonnaire P, Lancellotti P, Ajmone Marsan N, Tops LF, Min JK, et al. Transcatheter interventions for mitral regurgitation: multimodality imaging for patient selection and procedural guidance. *JACC Cardiovasc Imaging* 2019; **12**: 2029–48. doi: <https://doi.org/10.1016/j.jcmg.2019.03.036>
- Blanke P, Naoum C, Webb J, Dvir D, Hahn RT, Grayburn P, et al. Multimodality imaging in the context of transcatheter mitral valve replacement: establishing consensus among modalities and disciplines. *JACC Cardiovasc Imaging* 2015; **8**: 1191–208. doi: <https://doi.org/10.1016/j.jcmg.2015.08.004>
- Hahn RT, Nabauer M, Zuber M, Nazif TM, Hausleiter J, Taramasso M, et al. Intraprocedural imaging of transcatheter tricuspid valve interventions. *JACC Cardiovasc Imaging* 2019; **12**: 532–53. doi: <https://doi.org/10.1016/j.jcmg.2018.07.034>
- Zamorano JL, Badano LP, Bruce C, Chan K-L, Gonçalves A, Hahn RT, et al. EAE/ASE recommendations for the use of echocardiography in new transcatheter interventions for valvular heart disease. *J Am Soc Echocardiogr* 2011; **24**: 937–65. doi: <https://doi.org/10.1016/j.echo.2011.07.003>
- Mor-Avi V, Lang RM, Badano LP, Belohlavek M, Cardim NM, Derumeaux G, et al. Current and evolving echocardiographic techniques for the quantitative evaluation of cardiac mechanics: ASE/EAE consensus statement on methodology and indications endorsed by the Japanese Society of echocardiography. *J Am Soc Echocardiogr* 2011; **24**: 277–313. doi: <https://doi.org/10.1016/j.echo.2011.01.015>
- Thavendiranathan P, Poulin F, Lim K-D, Plana JC, Woo A, Marwick TH. Use of myocardial strain imaging by echocardiography for the early detection of cardiotoxicity in patients during and after cancer chemotherapy. *J Am Coll Cardiol* 2014; **63**: 2751–68. doi: <https://doi.org/10.1016/j.jacc.2014.01.073>
- Vollema EM, Sugimoto T, Shen M, Tastet L, Ng ACT, Abou R, et al. Association of left ventricular global longitudinal strain with asymptomatic severe aortic stenosis: natural course and prognostic value. *JAMA Cardiol* 2018; **3**: 839–47. doi: <https://doi.org/10.1001/jamacardio.2018.2288>
- Gorcsan J, Oyenuga O, Habib PJ, Tanaka H, Adelstein EC, Hara H, et al. Relationship of echocardiographic dyssynchrony to long-term survival after cardiac resynchronization therapy. *Circulation* 2010; **122**: 1910–8. doi: <https://doi.org/10.1161/CIRCULATIONAHA.110.954768>
- Delgado V, Bax JJ. Assessment of systolic dyssynchrony for cardiac resynchronization therapy is clinically useful. *Circulation* 2011; **123**: 640–55. doi: <https://doi.org/10.1161/CIRCULATIONAHA.110.954404>
- Ternacle J, Bodez D, Guellich A, Audureau E, Rappeneau S, Lim P, et al. Causes and consequences of longitudinal LV dysfunction assessed by 2D strain echocardiography in cardiac amyloidosis. *JACC Cardiovasc Imaging* 2016; **9**: 126–38. doi: <https://doi.org/10.1016/j.jcmg.2015.05.014>
- Pellikka PA, Arruda-Olson A, Chaudhry FA, Chen MH, Marshall JE, Porter TR, et al. Guidelines for performance, interpretation,

- and application of stress echocardiography in ischemic heart disease: from the American Society of echocardiography. *J Am Soc Echocardiogr* 2020; **33**: 1–41. doi: <https://doi.org/10.1016/j.echo.2019.07.001>
19. Kirkpatrick JN, Grimm R, Johri AM, Kimura BJ, Kort S, Labovitz AJ, et al. Recommendations for echocardiography laboratories participating in cardiac point of care cardiac ultrasound (POCUS) and critical care echocardiography training: report from the American Society of echocardiography. *J Am Soc Echocardiogr* 2020; **33**: 409–22. doi: <https://doi.org/10.1016/j.echo.2020.01.008>
 20. Johri AM, Galen B, Kirkpatrick JN, Lanspa M, Mulvagh S, Thamman R. Ase statement on point-of-care ultrasound during the 2019 novel coronavirus pandemic. *J Am Soc Echocardiogr* 2020; **33**: 670–3. doi: <https://doi.org/10.1016/j.echo.2020.04.017>
 21. Hsiao EM, Rybicki FJ, Steigner M. CT coronary angiography: 256-slice and 320-detector row scanners. *Curr Cardiol Rep* 2010; **12**: 68–75. doi: <https://doi.org/10.1007/s11886-009-0075-z>
 22. Min JK, Shaw LJ, Berman DS. The present state of coronary computed tomography angiography a process in evolution. *J Am Coll Cardiol* 2010; **55**: 957–65. doi: <https://doi.org/10.1016/j.jacc.2009.08.087>
 23. Fordyce CB, Douglas PS. Optimal non-invasive imaging test selection for the diagnosis of ischaemic heart disease. *Heart* 2016; **102**: 555–64. doi: <https://doi.org/10.1136/heartjnl-2015-307764>
 24. Lin FY, Shaw LJ, Dunning AM, Labounty TM, Choi J-H, Weinsaft JW, et al. Mortality risk in symptomatic patients with nonobstructive coronary artery disease: a prospective 2-center study of 2,583 patients undergoing 64-detector row coronary computed tomographic angiography. *J Am Coll Cardiol* 2011; **58**: 510–9. doi: <https://doi.org/10.1016/j.jacc.2010.11.078>
 25. Maddox TM, Stanislawski MA, Grunwald GK, Bradley SM, Ho PM, Tsai TT, et al. Nonobstructive coronary artery disease and risk of myocardial infarction. *JAMA* 2014; **312**: 1754–63. doi: <https://doi.org/10.1001/jama.2014.14681>
 26. Pagidipati NJ, Hemal K, Coles A, Mark DB, Dolor RJ, Pellikka PA, et al. Sex differences in functional and CT angiography testing in patients with suspected coronary artery disease. *J Am Coll Cardiol* 2016; **67**: 2607–16. doi: <https://doi.org/10.1016/j.jacc.2016.03.523>
 27. Motoyama S, Sarai M, Harigaya H, Anno H, Inoue K, Hara T, et al. Computed tomographic angiography characteristics of atherosclerotic plaques subsequently resulting in acute coronary syndrome. *J Am Coll Cardiol* 2009; **54**: 49–57. doi: <https://doi.org/10.1016/j.jacc.2009.02.068>
 28. Park H-B, Heo R, Ó Hartaigh B, Cho I, Gransar H, Nakazato R, et al. Atherosclerotic plaque characteristics by CT angiography identify coronary lesions that cause ischemia: a direct comparison to fractional flow reserve. *JACC Cardiovasc Imaging* 2015; **8**: 1–10. doi: <https://doi.org/10.1016/j.jcmg.2014.11.002>
 29. Ferencik M, Mayrhofer T, Bittner DO, Emami H, Puchner SB, Lu MT, et al. Use of high-risk coronary atherosclerotic plaque detection for risk stratification of patients with stable chest pain: a secondary analysis of the promise randomized clinical trial. *JAMA Cardiol* 2018; **3**: 144–52. doi: <https://doi.org/10.1001/jamacardio.2017.4973>
 30. Kolossváry M, Park J, Bang J-I, Zhang J, Lee JM, Paeng JC, et al. Identification of invasive and radionuclide imaging markers of coronary plaque vulnerability using radiomic analysis of coronary computed tomography angiography. *Eur Heart J Cardiovasc Imaging* 2019; **20**: 1250–8. doi: <https://doi.org/10.1093/ehjci/jez033>
 31. Den Harder AM, Willemink MJ, De Ruiter QMB, De Jong PA, Schilham AMR, Krestin GP, et al. Dose reduction with iterative reconstruction for coronary CT angiography: a systematic review and meta-analysis. *Br J Radiol* 2016; **89**: 20150068. doi: <https://doi.org/10.1259/bjr.20150068>
 32. Taylor CA, Fonte TA, Min JK. Computational fluid dynamics applied to cardiac computed tomography for noninvasive quantification of fractional flow reserve. *J Am Coll Cardiol* 2013; **61**: 2233–41. doi: <https://doi.org/10.1016/j.jacc.2012.11.083>
 33. Koo B-K, Erglis A, Doh J-H, Daniels DV, Jegere S, Kim H-S, et al. Diagnosis of ischemia-causing coronary stenoses by noninvasive fractional flow reserve computed from coronary computed tomographic angiograms. results from the prospective multicenter DISCOVER-FLOW (diagnosis of ischemia-causing stenoses obtained via noninvasive fractional flow reserve) study. *J Am Coll Cardiol* 2011; **58**: 1989–97. doi: <https://doi.org/10.1016/j.jacc.2011.06.066>
 34. Min JK, Leipsic J, Pencina MJ, Berman DS, Koo B-K, van Mieghem C, et al. Diagnostic accuracy of fractional flow reserve from anatomic CT angiography. *JAMA* 2012; **308**: 1237–45. doi: <https://doi.org/10.1001/2012.jama.11274>
 35. Nørgaard BL, Leipsic J, Gaur S, Seneviratne S, Ko BS, Ito H, et al. Diagnostic performance of noninvasive fractional flow reserve derived from coronary computed tomography angiography in suspected coronary artery disease: the NXT trial (analysis of coronary blood flow using CT angiography: next steps). *J Am Coll Cardiol* 2014; **63**: 1145–55. doi: <https://doi.org/10.1016/j.jacc.2013.11.043>
 36. Douglas PS, Pontone G, Hlatky MA, Patel MR, Nørgaard BL, Byrne RA, et al. Clinical outcomes of fractional flow reserve by computed tomographic angiography-guided diagnostic strategies vs. usual care in patients with suspected coronary artery disease: the prospective longitudinal trial of FFR_{CT}: outcome and resource impacts study. *Eur Heart J* 2015; **36**: 3359–67. doi: <https://doi.org/10.1093/eurheartj/ehv444>
 37. Patel MR, Nørgaard BL, Fairbairn TA, Nieman K, Akasaka T, Berman DS, et al. 1-Year impact on medical practice and clinical outcomes of FFR_{CT}. *JACC Cardiovasc Imaging* 2020; **13**: 97–105. doi: <https://doi.org/10.1016/j.jcmg.2019.03.003>
 38. Lee JM, Choi KH, Koo B-K, Park J, Kim J, Hwang D, et al. Prognostic implications of plaque characteristics and stenosis severity in patients with coronary artery disease. *J Am Coll Cardiol* 2019; **73**: 2413–24. doi: <https://doi.org/10.1016/j.jacc.2019.02.060>
 39. Gerber BL, Belge B, Legros GJ, Lim P, Poncelet A, Pasquet A, et al. Characterization of acute and chronic myocardial infarcts by multidetector computed tomography: comparison with contrast-enhanced magnetic resonance. *Circulation* 2006; **113**: 823–33. doi: <https://doi.org/10.1161/CIRCULATIONAHA.104.529511>
 40. Celeng C, Leiner T, Maurovich-Horvat P, Merkely B, de Jong P, Dankbaar JW, et al. Anatomical and functional computed tomography for diagnosing Hemodynamically significant coronary artery disease: a meta-analysis. *JACC Cardiovasc Imaging* 2019; **12**(7 Pt 2): 1316–25. doi: <https://doi.org/10.1016/j.jcmg.2018.07.022>
 41. Takx RAP, Blomberg BA, Aidi HE, Habets J, de Jong PA, Nagel E, et al. Diagnostic accuracy of stress myocardial perfusion imaging compared to invasive coronary angiography with fractional flow reserve meta-analysis. *Circulation* 2015; **8**. doi: <https://doi.org/10.1161/CIRCIMAGING.114.002666>
 42. Salgado RA, Leipsic JA, Shivalkar B, Ardies L, Van Herck PL, Op de Beeck BJ, et al. Preprocedural CT evaluation of

- transcatheter aortic valve replacement: what the radiologist needs to know. *RadioGraphics* 2014; **34**: 1491–514. doi: <https://doi.org/10.1148/rg.346125076>
43. Hansson NC, Grove EL, Andersen HR, Leipsic J, Mathiassen ON, Jensen JM, et al. Transcatheter aortic valve thrombosis: incidence, predisposing factors, and clinical implications. *J Am Coll Cardiol* 2016; **68**: 2059–69. doi: <https://doi.org/10.1016/j.jacc.2016.08.010>
 44. Andrews JPM, Cartlidge TR, Dweck MR, Moss AJ. Cardiac CT in prosthetic aortic valve complications. *Br J Radiol* 2019; **92**: 20180237. doi: <https://doi.org/10.1259/bjr.20180237>
 45. Blanke P, Weir-McCall JR, Achenbach S, Delgado V, Hausleiter J, Jilaihawi H, et al. Computed tomography imaging in the context of transcatheter aortic valve implantation (TAVI)/transcatheter aortic valve replacement (TAVR): an expert consensus document of the society of cardiovascular computed tomography. *JACC Cardiovasc Imaging* 2019; **12**: 1–24. doi: <https://doi.org/10.1016/j.jcmg.2018.12.003>
 46. Naoum C, Blanke P, Cavalante JL, Leipsic J. Cardiac computed tomography and magnetic resonance imaging in the evaluation of mitral and tricuspid valve disease: implications for transcatheter interventions. *Circ Cardiovasc Imaging* 2017; **10**: e005331. doi: <https://doi.org/10.1161/CIRCIMAGING.116.005331>
 47. Mooney J, Sellers SL, Blanke P, Pibarot P, Hahn RT, Dvir D, et al. CT-defined prosthesis-patient mismatch downgrades frequency and severity, and demonstrates no association with adverse outcomes after transcatheter aortic valve replacement. *JACC Cardiovasc Interv* 2017; **10**: 1578–87. doi: <https://doi.org/10.1016/j.jcin.2017.05.031>
 48. Blanke P, Pibarot P, Hahn R, Weissman N, Kodali S, Thourani V, et al. Computed tomography-based oversizing degrees and incidence of paravalvular regurgitation of a new generation transcatheter heart valve. *JACC Cardiovasc Interv* 2017; **10**: 810–20. doi: <https://doi.org/10.1016/j.jcin.2017.02.021>
 49. Ismail TF, Panikker S, Markides V, Foran JP, Padley S, Rubens MB, et al. CT imaging for left atrial appendage closure: a review and pictorial essay. *J Cardiovasc Comput Tomogr* 2015; **9**: 89–102. doi: <https://doi.org/10.1016/j.jcct.2015.01.011>
 50. Mittal TK, Panicker MG, Mitchell AG, Banner NR. Cardiac allograft vasculopathy after heart transplantation: electrocardiographically gated cardiac CT angiography for assessment. *Radiology* 2013; **268**: 374–81. doi: <https://doi.org/10.1148/radiol.13121440>
 51. Patel PA, Green CL, Lokhnygina Y, Christensen J, Milano CA, Rogers JG, et al. Cardiac computed tomography improves the identification of cardiomechanical complications among patients with suspected left ventricular assist device malfunction. *J Cardiovasc Comput Tomogr* 2020; **28** Aug 2020. doi: <https://doi.org/10.1016/j.jcct.2020.08.008>
 52. Kilner PJ, Geva T, Kaemmerer H, Trindade PT, Schwitter J, Webb GD. Recommendations for cardiovascular magnetic resonance in adults with congenital heart disease from the respective working groups of the European Society of cardiology. *Eur Heart J* 2010; **31**: 794–805. doi: <https://doi.org/10.1093/eurheartj/ehp586>
 53. Bogaert J, Francone M. Cardiovascular magnetic resonance in pericardial diseases. *J Cardiovasc Magn Reson* 2009; **11**: 14. doi: <https://doi.org/10.1186/1532-429X-11-14>
 54. Fussen S, De Boeck BWL, Zellweger MJ, Bremerich J, Goetschalckx K, Zuber M, et al. Cardiovascular magnetic resonance imaging for diagnosis and clinical management of suspected cardiac masses and tumours. *Eur Heart J* 2011; **32**: 1551–60. doi: <https://doi.org/10.1093/eurheartj/ehr104>
 55. Alfakih K, Reid S, Jones T, Sivananthan M. Assessment of ventricular function and mass by cardiac magnetic resonance imaging. *Eur Radiol* 2004; **14**: 1813–22. doi: <https://doi.org/10.1007/s00330-004-2387-0>
 56. Bruder O, Wagner A, Lombardi M, Schwitter J, van Rossum A, Pilz G, et al. European cardiovascular magnetic resonance (EuroCMR) registry – multi national results from 57 centers in 15 countries. *J Cardiovasc Magn Reson* 2013; **15**: 9. doi: <https://doi.org/10.1186/1532-429X-15-9>
 57. Cummings KW, Bhalla S, Javidan-Nejad C, Bierhals AJ, Gutierrez FR, Woodard PK. A pattern-based approach to assessment of delayed enhancement in nonischemic cardiomyopathy at MR imaging. *RadioGraphics* 2009; **29**: 89–103. doi: <https://doi.org/10.1148/rg.291085052>
 58. Bohnen S, Radunski UK, Lund GK, Kandolf R, Stehning C, Schnackenburg B, et al. Performance of T1 and T2 mapping cardiovascular magnetic resonance to detect active myocarditis in patients with recent-onset heart failure. *Circ Cardiovasc Imaging* 2015; **8**: e003073. doi: <https://doi.org/10.1161/CIRCIMAGING.114.003073>
 59. Lurz P, Luecke C, Eitel I, Föhrenbach F, Frank C, Grothoff M, et al. Comprehensive cardiac magnetic resonance imaging in patients with suspected myocarditis. *J Am Coll Cardiol* 2016; **67**: 1800–11. doi: <https://doi.org/10.1016/j.jacc.2016.02.013>
 60. Pan JA, Lee YJ, Salerno M. Diagnostic performance of extracellular volume, native T1, and T2 mapping versus lake Louise criteria by cardiac magnetic resonance for detection of acute myocarditis. *Circulation* 2018; **111**: e007598. doi: <https://doi.org/10.1161/CIRCIMAGING.118.007598>
 61. Karamitsos TD, Piechnik SK, Banyersad SM, Fontana M, Ntusi NB, Ferreira VM, et al. Noncontrast T1 mapping for the diagnosis of cardiac amyloidosis. *JACC Cardiovasc Imaging* 2013; **6**: 488–97. doi: <https://doi.org/10.1016/j.jcmg.2012.11.013>
 62. Tang CX, Petersen SE, Sanghvi MM, Lu GM, Zhang LJ. Cardiovascular magnetic resonance imaging for amyloidosis: the state-of-the-art. *Trends Cardiovasc Med* 2019; **29**: 83–94. doi: <https://doi.org/10.1016/j.tcm.2018.06.011>
 63. Chaikriangkrai K, Abbasi MA, Sarnari R, Dolan R, Lee D, Anderson AS, et al. Prognostic value of myocardial extracellular volume fraction and T2-mapping in heart transplant patients. *JACC Cardiovasc Imaging* 2020; **13**: 1521–30. doi: <https://doi.org/10.1016/j.jcmg.2020.01.014>
 64. Hinojar R, Varma N, Child N, Goodman B, Jabbour A, Yu C-Y, et al. T1 mapping in discrimination of hypertrophic phenotypes: hypertensive heart disease and hypertrophic cardiomyopathy: findings from the International T1 multicenter cardiovascular magnetic resonance study. *Circ Cardiovasc Imaging* 2015; **8**: e003285. doi: <https://doi.org/10.1161/CIRCIMAGING.115.003285>
 65. Messroghli DR, Moon JC, Ferreira VM, Grosse-Wortmann L, He T, Kellman P, et al. Clinical recommendations for cardiovascular magnetic resonance mapping of T1, T2, T2* and extracellular volume: a consensus statement by the Society for cardiovascular magnetic resonance (SCMR) endorsed by the European association for cardiovascular imaging (EACVI). *J Cardiovasc Magn Reson* 2017; **19**: 75. doi: <https://doi.org/10.1186/s12968-017-0389-8>
 66. Kim RJ, Wu E, Rafael A, Chen E-L, Parker MA, Simonetti O, et al. The use of contrast-enhanced magnetic resonance imaging to identify reversible myocardial dysfunction. *N Engl J Med Overseas Ed* 2000; **343**: 1445–53. doi: <https://doi.org/10.1056/NEJM200011163432003>
 67. Ordovas KG, Higgins CB. Delayed contrast enhancement on Mr images of myocardium:

- past, present, future. *Radiology* 2011; **261**: 358–74. doi: <https://doi.org/10.1148/radiol.11091882>
68. Shan K, Constantine G, Sivananthan M, Flamm SD. Role of cardiac magnetic resonance imaging in the assessment of myocardial viability. *Circulation* 2004; **109**: 1328–34. doi: <https://doi.org/10.1161/01.CIR.0000120294.67948.E3>
 69. Kwong RY, Ge Y, Steel K, Bingham S, Abdullah S, Fujikura K, et al. Cardiac Magnetic Resonance Stress Perfusion Imaging for Evaluation of Patients With Chest Pain. *J Am Coll Cardiol* 2019; **74**: 1741–55. doi: <https://doi.org/10.1016/j.jacc.2019.07.074>
 70. Greenwood JP, Maredia N, Younger JF, Brown JM, Nixon J, Everett CC, et al. Cardiovascular magnetic resonance and single-photon emission computed tomography for diagnosis of coronary heart disease (CE-MARC): a prospective trial. *The Lancet* 2012; **379**: 453–60. doi: [https://doi.org/10.1016/S0140-6736\(11\)61335-4](https://doi.org/10.1016/S0140-6736(11)61335-4)
 71. Nagel E, Greenwood JP, McCann GP, Bettencourt N, Shah AM, Hussain ST, et al. Magnetic resonance perfusion or fractional flow reserve in coronary disease. *New England Journal of Medicine* 2019; **380**: 2418–28. doi: <https://doi.org/10.1056/NEJMoa1716734>
 72. Mauricio R, Srichai MB, Axel L, Hochman JS, Reynolds HR. Stress cardiac MRI in women with myocardial infarction and nonobstructive coronary artery disease. *Clin Cardiol* 2016; **39**: 596–602. doi: <https://doi.org/10.1002/clc.22571>
 73. Dastidar AG, Rodrigues JCL, Johnson TW, De Garate E, Singhal P, Baritussio A, et al. Myocardial infarction with nonobstructed arteries: impact of CMR early after presentation. *JACC Cardiovasc Imaging* 2017; **10**(10 Pt A): 1204–6. doi: <https://doi.org/10.1016/j.jcmg.2016.11.010>
 74. Klein-Wiele O, Garmer M, Busch M, Mateiescu S, Urbien R, Barbone G, et al. Cardiovascular magnetic resonance in patients with magnetic resonance conditional pacemaker systems at 1.5 T: influence of pacemaker related artifacts on image quality including first pass perfusion, aortic and mitral valve assessment, flow measurement, short tau inversion recovery and T1-weighted imaging. *Int J Cardiovasc Imaging* 2017; **33**: 383–94. doi: <https://doi.org/10.1007/s10554-016-1012-z>
 75. Tan LK, McLaughlin RA, Lim E, Abdul Aziz YF, Liew YM. Fully automated segmentation of the left ventricle in cine cardiac MRI using neural network regression. *J Magn Reson Imaging* 2018; **48**: 140–52. doi: <https://doi.org/10.1002/jmri.25932>
 76. Zhang N, Yang G, Gao Z, Xu C, Zhang Y, Shi R, et al. Deep learning for diagnosis of chronic myocardial infarction on Nonenhanced cardiac cine MRI. *Radiology* 2019; **291**: 606–17. doi: <https://doi.org/10.1148/radiol.2019182304>
 77. Klocke FJ, Baird MG, Lorell BH, Bateman TM, Messer JV, Berman DS, et al. ACC/AHA/ASNC guidelines for the clinical use of cardiac radionuclide imaging-executive summary: a report of the American College of Cardiology/American Heart association task force on practice guidelines (ACC/AHA/ASNC committee to revise the 1995 guidelines for the clinical use of cardiac radionuclide imaging. *J Am Coll Cardiol* 2003; **42**: 1318–33. doi: <https://doi.org/10.1016/j.jacc.2003.08.011>
 78. Duvall WL, Guma KA, Kamen J, Croft LB, Parides M, George T, et al. Reduction in occupational and patient radiation exposure from myocardial perfusion imaging: impact of stress-only imaging and high-efficiency SPECT camera technology. *J Nucl Med* 2013; **54**: 1251–7. doi: <https://doi.org/10.2967/jnumed.112.112680>
 79. Einstein AJ, Johnson LL, DeLuca AJ, Kontak AC, Groves DW, Stant J, et al. Radiation dose and prognosis of ultra-low-dose stress-first myocardial perfusion SPECT in patients with chest pain using a high-efficiency camera. *J Nucl Med* 2015; **56**: 545–51. doi: <https://doi.org/10.2967/jnumed.114.150664>
 80. Depuey EG. New software methods to cope with reduced counting statistics: shorter SPECT acquisitions and many more possibilities. *J Nucl Cardiol* 2009; **16**: 335–8. doi: <https://doi.org/10.1007/s12350-009-9079-8>
 81. Yoshinaga K, Katoh C, Noriyasu K, Iwado Y, Furuyama H, Ito Y, et al. Reduction of coronary flow reserve in areas with and without ischemia on stress perfusion imaging in patients with coronary artery disease: a study using oxygen 15-labeled water PET. *J Nucl Cardiol* 2003; **10**: 275–83. doi: [https://doi.org/10.1016/S1071-3581\(02\)43243-6](https://doi.org/10.1016/S1071-3581(02)43243-6)
 82. Bengel FM, Higuchi T, Javadi MS, Lautamäki R. Cardiac positron emission tomography. *J Am Coll Cardiol* 2009; **54**: 1–15. doi: <https://doi.org/10.1016/j.jacc.2009.02.065>
 83. Schindler TH, Schelbert HR, Quercioli A, Dilsizian V. Cardiac PET imaging for the detection and monitoring of coronary artery disease and microvascular health. *JACC Cardiovasc Imaging* 2010; **3**: 623–40. doi: <https://doi.org/10.1016/j.jcmg.2010.04.007>
 84. Sdringola S, Nakagawa K, Nakagawa Y, Yusuf SW, Boccalandro F, Mullani N, et al. Combined intense lifestyle and pharmacologic lipid treatment further reduce coronary events and myocardial perfusion abnormalities compared with usual-care cholesterol-lowering drugs in coronary artery disease. *J Am Coll Cardiol* 2003; **41**: 263–72. doi: [https://doi.org/10.1016/S0735-1097\(02\)02693-1](https://doi.org/10.1016/S0735-1097(02)02693-1)
 85. Schinkel AFL, Bax JJ, Poldermans D, Elhendy A, Ferrari R, Rahimtoola SH. Hibernating myocardium: diagnosis and patient outcomes. *Curr Probl Cardiol* 2007; **32**: 375–410. doi: <https://doi.org/10.1016/j.cpcardiol.2007.04.001>
 86. Sasano T, Abraham MR, Chang K-C, Ashikaga H, Mills KJ, Holt DP, et al. Abnormal sympathetic innervation of viable myocardium and the substrate of ventricular tachycardia after myocardial infarction. *J Am Coll Cardiol* 2008; **51**: 2266–75. doi: <https://doi.org/10.1016/j.jacc.2008.02.062>
 87. Dilsizian V, Eckelman WC, Loreda ML, Jagoda EM, Shirani J. Evidence for tissue angiotensin-converting enzyme in explanted hearts of ischemic cardiomyopathy using targeted radiotracer technique. *J Nucl Med* 2007; **48**: 182–7.
 88. Davies JR, Rudd JF, Fryer TD, Weissberg PL. Targeting the vulnerable plaque: the evolving role of nuclear imaging. *J Nucl Cardiol* 2005; **12**: 234–46. doi: <https://doi.org/10.1016/j.nuclcard.2005.01.008>
 89. Singh V, Falk R, Di Carli MF, Kijewski M, Rapezzi C, Dorbala S. State-of-the-art radionuclide imaging in cardiac transthyretin amyloidosis. *J Nucl Cardiol* 2019; **26**: 158–73. doi: <https://doi.org/10.1007/s12350-018-01552-4>
 90. Castano A, Haq M, Narotsky DL, Goldsmith J, Weinberg RL, Morgenstern R, et al. Multicenter study of planar technetium 99m pyrophosphate cardiac imaging: predicting survival for patients with ATTR cardiac amyloidosis. *JAMA Cardiol* 2016; **1**: 880–9. doi: <https://doi.org/10.1001/jamacardio.2016.2839>
 91. Boden WE, O'Rourke RA, Teo KK, Hartigan PM, Maron DJ, Kostuk WJ, et al. Optimal medical therapy with or without PCI for stable coronary disease. *N Engl J Med Overseas Ed* 2007; **356**: 1503–16. doi: <https://doi.org/10.1056/NEJMoa070829>
 92. Frye RL, August P, Brooks MM, Hardison RM, Kelsey SF, et al. A randomized trial of therapies for type 2 diabetes and coronary artery disease. *N Engl J Med* 2009; **360**:

- 2503–15. doi: <https://doi.org/10.1056/NEJMoa0805796>
93. De Bruyne B, Pijls NHJ, Kalesan B, Barbato E, Tonino PAL, Piroth Z, et al. Fractional flow reserve-guided PCI versus medical therapy in stable coronary disease. *N Engl J Med* 2012; **367**: 991–1001. doi: <https://doi.org/10.1056/NEJMoa1205361>
 94. Gaemperli O, Schepis T, Valenta I, Koepfli P, Husmann L, Scheffel H, et al. Functionally relevant coronary artery disease: comparison of 64-section CT angiography with myocardial perfusion SPECT. *Radiology* 2008; **248**: 414–23. doi: <https://doi.org/10.1148/radiol.2482071307>
 95. Tonino PAL, De Bruyne B, Pijls NHJ, Siebert U, Ikeno F, van't Veer M, et al. Fractional flow reserve versus angiography for guiding percutaneous coronary intervention. *N Engl J Med* 2009; **360**: 213–24. doi: <https://doi.org/10.1056/NEJMoa0807611>
 96. Flotats A, Knuuti J, Gutberlet M, Marcassa C, Bengel FM, Kaufmann PA, et al. Hybrid cardiac imaging: SPECT/CT and PET/CT. A joint position statement by the European association of nuclear medicine (EANM), the European Society of cardiac radiology (ESCR) and the European Council of nuclear cardiology (ECNC). *Eur J Nucl Med Mol Imaging* 2011; **38**: 201–12. doi: <https://doi.org/10.1007/s00259-010-1586-y>
 97. Pazhenkottil AP, Nkoulou RN, Ghadri J-R, Herzog BA, Buechel RR, Kuest SM, et al. Prognostic value of cardiac hybrid imaging integrating single-photon emission computed tomography with coronary computed tomography angiography. *Eur Heart J* 2011; **32**: 1465–71. doi: <https://doi.org/10.1093/eurheartj/ehr047>
 98. Bavishi C, Argulian E, Chatterjee S, Rozanski A. CACS and the frequency of stress-induced myocardial ischemia during MPI: a meta-analysis. *JACC Cardiovasc Imaging* 2016; **9**: 580–9. doi: <https://doi.org/10.1016/j.jcmg.2015.11.023>
 99. Liga R, Vontobel J, Rovai D, Marinelli M, Caselli C, Pietila M, et al. Multicentre multi-device hybrid imaging study of coronary artery disease: results from the evaluation of integrated cardiac imaging for the detection and characterization of ischaemic heart disease (EVINCI) hybrid imaging population. *Eur Heart J Cardiovasc Imaging* 2016; **17**: 951–60. doi: <https://doi.org/10.1093/ehjci/jew038>
 100. Javadi MS, Lautamäki R, Merrill J, Voicu C, Epley W, McBride G, et al. Definition of vascular territories on myocardial perfusion images by integration with true coronary anatomy: a hybrid PET/CT analysis. *J Nucl Med* 2010; **51**: 198–203. doi: <https://doi.org/10.2967/jnumed.109.067488>
 101. Ratib O, Nkoulou R. Potential applications of PET/MR imaging in cardiology. *J Nucl Med* 2014; **55**(Supplement 2): 40S–6. doi: <https://doi.org/10.2967/jnumed.113.129262>
 102. van der Hoeven BL, Schaliij MJ, Delgado V. Multimodality imaging in interventional cardiology. *Nat Rev Cardiol* 2012; **9**: 333–46. doi: <https://doi.org/10.1038/nrcardio.2012.14>
 103. Faletta FF, Biasco L, Pedrazzini G, Moccetti M, Pasotti E, Leo LA, et al. Echocardiographic-fluoroscopic fusion imaging in transseptal puncture: a new technology for an old procedure. *J Am Soc Echocardiogr* 2017; **30**: 886–95. doi: <https://doi.org/10.1016/j.echo.2017.05.001>
 104. Kliger C, Jelnin V, Sharma S, Panagopoulos G, Einhorn BN, Kumar R, et al. CT angiography-fluoroscopy fusion imaging for percutaneous transapical access. *JACC Cardiovasc Imaging* 2014; **7**: 169–77. doi: <https://doi.org/10.1016/j.jcmg.2013.10.009>
 105. Syros GOM. Advances in imaging to assist atrial fibrillation ablation. *J Innov Card Rhythm Manag* 2011; **2**: 570–82. doi: <https://doi.org/10.19102/icrm.2011.021204>
 106. Dey D, Slomka PJ, Leeson P, Comaniciu D, Shrestha S, Sengupta PP, et al. Artificial intelligence in cardiovascular imaging: JACC state-of-the-art review. *J Am Coll Cardiol* 2019; **73**: 1317–35. doi: <https://doi.org/10.1016/j.jacc.2018.12.054>
 107. Al'Aref SJ, Anchouche K, Singh G, Slomka PJ, Kolli KK, Kumar A, et al. Clinical applications of machine learning in cardiovascular disease and its relevance to cardiac imaging. *Eur Heart J* 2019; **40**: 1975–86. doi: <https://doi.org/10.1093/eurheartj/ehy404>
 108. Winther HB, Hundt C, Schmidt B, Czerner C, Bauersachs J, Wacker F, et al. v-net: deep learning for generalized biventricular mass and function parameters using multicenter cardiac MRI data. *JACC Cardiovasc Imaging* 2018; **11**: 1036–8. doi: <https://doi.org/10.1016/j.jcmg.2017.11.013>
 109. Ernande L, Audureau E, Jellis CL, Bergerot C, Henegar C, Sawaki D, et al. Clinical implications of echocardiographic phenotypes of patients with diabetes mellitus. *J Am Coll Cardiol* 2017; **70**: 1704–16. doi: <https://doi.org/10.1016/j.jacc.2017.07.792>
 110. Zreik M, Lessmann N, van Hamersvelt RW, Wolterink JM, Voskuil M, Viergever MA, et al. Deep learning analysis of the myocardium in coronary CT angiography for identification of patients with functionally significant coronary artery stenosis. *Med Image Anal* 2018; **44**: 72–85. doi: <https://doi.org/10.1016/j.media.2017.11.008>
 111. Motwani M, Dey D, Berman DS, Germano G, Achenbach S, Al-Mallah MH, et al. Machine learning for prediction of all-cause mortality in patients with suspected coronary artery disease: a 5-year multicentre prospective registry analysis. *Eur Heart J* 2017; **38**: 500–7. doi: <https://doi.org/10.1093/eurheartj/ehw188>
 112. Betancur J, Commandeur F, Motlagh M, Sharir T, Einstein AJ, Bokhari S, et al. Deep learning for prediction of obstructive disease from fast myocardial perfusion SPECT: a multicenter study. *JACC Cardiovasc Imaging* 2018; **11**: 1654–63. doi: <https://doi.org/10.1016/j.jcmg.2018.01.020>